

Formation Dynamics and Conversion Efficiency of Micro-resonator Kerr Frequency Comb

SUNJIN CHOI¹

¹ University of Berkeley, California

* Corresponding author: sunjin_choi@berkeley.edu

Compiled December 16, 2022

In this letter, we study the formation dynamics and conversion efficiency of micro-resonator Kerr frequency comb using open-source pyLLE simulator. Using a simulator, we first simulate the dynamics of soliton generation from laser scanning transient simulation and verified primary comb-MI-DKS step transitions in the simulator. Furthermore, we explore the design space of Kerr comb, focusing on pump laser intensity and coupling coefficient. It is shown that resonator over-coupling and minimizing pump laser intensity would help conversion efficiency which has been one of the limiting factors of Kerr comb's mainstream adoption. © 2022 Optica Publishing Group

<http://dx.doi.org/10.1364/ao.XX.XXXXXX>

1. INTRODUCTION

Recent breakthroughs in micro-resonator Kerr soliton comb generation is gaining widespread attention from inside and outside of the optics community [1–3]. First and foremost would be the demystification of formation dynamics [4–6] in which multiple research institutes and universities have worked on step-by-step, from formation process breakdown, physical interpretations and lab measurements. Also, people have been bringing in the concept and design to the chip-scale fabrications [3, 7, 8] where compact form-factor and economical upscaling are both possible. The research area is gradually embarking on the mainstream industry these days, ranging from application-driven and large-scale demonstrations [9–12]. Researches on application-specific optimizations are also underway that would prove the feasibility of low-cost high-end comb lasers in the near future.

Spectrum of research in Kerr-microcomb generation during the past decade spans identifying the underlying mechanisms, overcoming the performance barriers, material engineering and penetration into foundry-compatible platforms and demonstration with the real-world applications. Nowadays the mechanism is well-known to be governed by the Lugiato-Lefever Equation (LLE) equation with diverse interactions between optical parametric processes like FWM, microring dynamics, soliton formation and thermal/Kerr-induced bistability [2, 4–6]. Also, key metrics such as comb bandwidth, pump-to-comb conversion power efficiency, power per comb line, operation simplicity

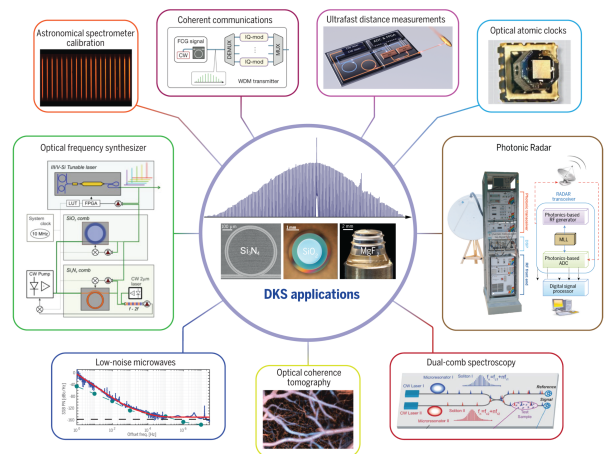


Fig. 1. Potential application area of Kerr frequency comb. Adopted from [2].

which barred Kerr comb's adoption have been significantly improved over the past decade [1]. Moreover, with the advent of chip-scale photonics, people have been actively looking for ways to miniaturize the device size and aligning the fabrication steps with CMOS foundry processes to leverage its unique advantages [3]. Finally, two of the most promising application areas, high-speed data communication and frequency metrology have been recently demonstrated [12, 13].

As it can act as an optical source empowering the diverse optics-based systems, its unique nature of wide-band, multi-wavelength and coherency can unlock the potentials of current systems (Figure 1) [1]. For example, wavelength-division multiplexed (WDM) data communication has multiple hurdles to overcome, one of which is wavelength count scalability and it poses challenges on a more prevalent DFB laser array. Also, wide-span and coherent comb tones could enable precision optical frequency metrology and synthesizer for atomic clocks and RF-to-optical communication. Furthermore, its low noise characteristics and phase coherence is likely to provide more opportunities for next-generation LIDAR with newly proposed dual microcomb.

While metrics like repetition rate, comb span, noise, operation simplicity and reliability are prime quality factors of comb lasers,

specifications related to optical power are worth highlighting as it is gating the widespread adoption of Kerr microcombs. Specifically, pump-to-comb conversion efficiency is one of the critical factors when used for data communications since it is linked to total power budgeting and feasibility in chip-scale implementations [1, 3, 10, 13]. However, to date 1~5% has been the nominal ballpark for Kerr comb conversion efficiencies which would require $>1\text{W}$ into a comb laser chip to get $>1\text{mW}$ power per comb line. Therefore, it calls for innovative designs like dark soliton (or platicon) based frequency comb [14, 15] or aggressive design space exploration of material and micro-resonator geometry parameters [7, 16, 17].

In this letter, we simulate the dynamics of Kerr comb formation and calculate the conversion efficiency of example micro-resonator Kerr frequency comb. We use the pyLLE package [18], an open-source Kerr frequency comb simulator with python interface and julia backend. Using the simulator, we also navigate the Kerr comb design space by sweeping pump laser power and micro-resonator-to-waveguide coupling to observe the dependence to the formation dynamics and conversion efficiency. Furthermore, we simulate over-coupled micro-resonators and extract coupling Q-to-conversion efficiency graph and verify that strong overcoupling can potentially achieve higher conversion efficiency.

2. PROBLEM STATEMENT

It is well-known that the governing equation of Kerr comb formation inside the micro-ring is the LLE equation, a mean-field damped driven NLS with Kerr nonlinearity and second order GVD [2]. The equation immediately implies the existence of dissipative Kerr solitons which is also a solution of a damped driven Nonlinear Schrodinger equation (NLS), and most of the studies on dissipative Kerr solitons and Kerr comb were based off a bulk literature on NLS in nonlinear optics. However, while it can serve as a governing equation of optical field dynamics, it can give a little insight into how a soliton can be generated, accessed and stabilized unless a thorough numerical simulation is accompanied. To the end, the research community has been iterating between numerical simulations and lab verifications to divide the soliton dynamics into multiple comprehensible phases and connect between the master equation and the soliton formation process [4–6].

Numerous studies have been done to understand the dynamics of Kerr soliton/comb formation. Kippenberg group has published a series of papers [4–6] which is marked as one of the seminal work in the area which divided the formation into multiple discrete steps. As from Fig 2, CW laser supplies a single optical tone into a micro-cavity. Typical way to initiate the soliton formation is to scan the laser wavelength from blue-side to red-side with respect to the cavity resonance wavelength. At blue-side detune, internal optical waves undergo degenerate/non-degenerate four-wave-mixing processes and create multiple primary sidebands or “Primary combs”. Then, triggered by micro-cavity round trips and self-reinforcing, optical waves undergo another set of parametric processes and creates smaller sidebands spaced by micro-cavity free-spectral-range (FSR) or “Secondary subcombs”. As laser wavelength approaches the cavity resonance, vast number of combs from parametric processes start to merge but in an incoherent form such that the overall waveform is noisy and unstable, or also known as “Modulation Instability”. Past the cavity resonance, when laser wavelength reaches the red-side detune, it accesses bistabil-

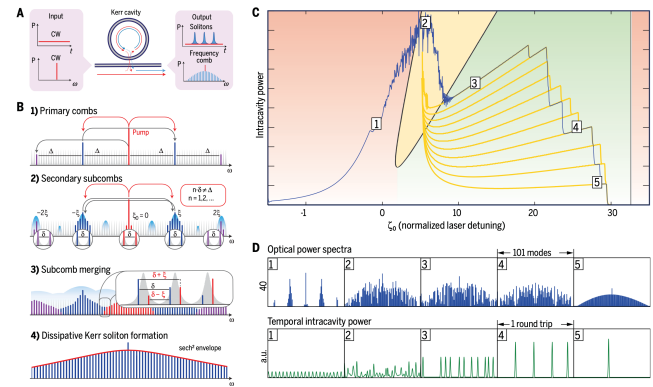


Fig. 2. Formation dynamics of dissipative Kerr solitons and Kerr frequency comb. Adopted from [2].

ity region and forms stable dissipative Kerr solitons (DKS) with blue-detuned solitons and red-detuned CW background. There, DKS maintains balances between parametric gain-resonator loss and dispersion-Kerr nonlinearity, while it is also known that blue-detuned solitons are high-power optical wavepackets that dominate the thermal response of the cavity thus maintaining effectively blue-detuned state which is thermally stable at red-detune.

While above complex dynamics cannot be reduced to a single closed-form equation without asymptotic approximations, numerical simulations attain as a necessity for analysis and design explorations. Model-based analysis can provide a useful insight into design guidelines, in particular to scaling laws of various parameters like comb span [19], conversion efficiency [17, 19] and cavity FSR [20]. However, it is usually backed by a full time-domain simulator to verify the claim and obtain a detailed guideline to achieve a target specification [2]. It is also useful to have a full transient laser scanning simulation as a ground truth of numerical estimation, yet to be verified by the actual measurements, but has a capability of demonstrating a soliton/comb formation at a specified design parameters.

Another aspect that we focus on in this letter is the conversion efficiency from pump laser power to comb [1, 13, 17]. As was discussed previously, conversion efficiency is one of the most important specifications of comb lasers in data communication and chip-scale integration. Since Kerr comb typically suffers from low conversion efficiency and at the same time, sensitive to the pump/cavity design parameters, it is essential to see what design guidelines can be provided for achieving a better conversion efficiency.

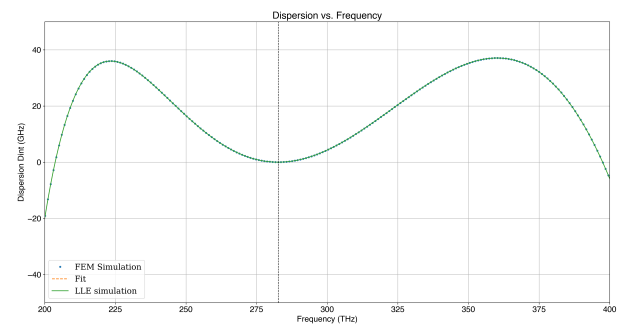


Fig. 3. Dispersion profile used for the simulation.

3. SIMULATOR

We use pyLLE [18], a python-interface and julia-backend open-source DKS simulator targeting both ease-of-use and faster performance. Solving the NLS equation includes a split-step Fourier method at the least, micro-resonator only aggravates the simulation complexity with added resonator couplings and round-trips. It is desirable to leverage the existing simulator and pyLLE's simple interface with its inherent compatibility with python is an attractive solution for wide-range of applications. Also, the software claims to be 2x faster than Matlab with its Julia engine.

Using pyLLE, we simulated the formation dynamics of solitons in a micro-resonator and analyzed conversion efficiency at different pump laser power, resonator coupling conditions. Nominal simulation parameters are shown in Table 1, including cavity radius, cavity intrinsic quality factor, cavity coupling quality factor, Kerr coefficient, pump laser power and pump laser frequency. Also, the dispersion profile used is shown in Fig 3. With nominal parameters, resulting laser scanning simulation is shown in Fig 4 with soliton state annotations.

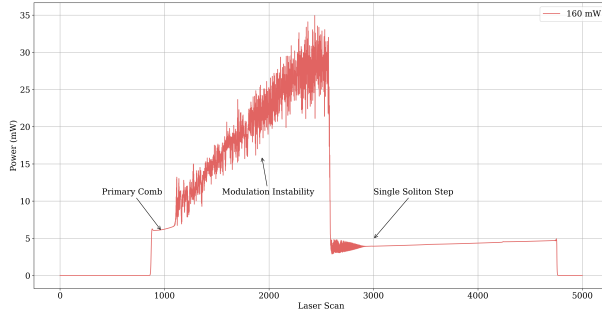


Fig. 4. Example soliton comb formation dynamics from laser scanning simulation. Laser scans from blue side to red side of resonator frequency. It first generates primary combs, followed by modulation instability at near cavity resonance, then collapse into a single or multiple soliton state indicated by discrete transitions.

4. RESULTS

We first simulate comb generation and spectrum at different pump power, coupling conditions. (Figure 5) Left panels show laser scanning simulations for both cases and right panels show comb output spectrum, while top panels correspond to pump power sweep and bottom to coupling Q sweep. It is apparent

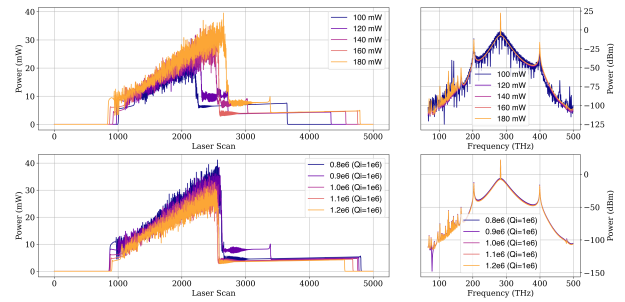


Fig. 5. (Left) Soliton formation dynamics at laser scan vs. pump laser power P_{in} and coupling quality factor Q_c (Right) Comb output spectrum at Laser scan 3600 (single soliton state) vs. pump laser power P_{in} and coupling quality factor Q_c .

that with different pump laser or cavity parameters, soliton formation can appear in a similar shape but in quite different scanning positions. Moreover, specifically for coupling coefficient sweep, the more the ring is over-coupled, the higher power the comb gets. Also two-soliton state is only accessed at $Q_c = 0.8M$ but not the other cases.

Next, Fig 6 compares the conversion efficiency at different pump power and coupling conditions. Conversion efficiency is calculated by probing at a specific laser scan time from the transient simulation and summing the comb tones minus the tone directly coupled from the pump and taking a ratio with the pump power. Pump power to conversion efficiency sweep is plotted at the left side of Fig. 6, showing a monotonic decrease in efficiency with input pump power. It is worth comparing with the simple analytical equation of pump-to-soliton conversion efficiency from [17] (Eq 1), where η is pump-to-soliton power ratio, θ input coupling coefficient, α half the round trip loss, β_2 and γ are the GVD and Kerr coefficients, P_{in} the pump power.

$$\eta = \frac{2\pi\theta^{3/2}}{\theta + \alpha L} \sqrt{\frac{|\beta_2|}{\gamma P_{in}}} \cdot FSR \quad (1)$$

As is the case of equation, conversion efficiency is monotonically decreasing with the pump power increase. Also, coupling condition to conversion efficiency is shown at the right side of Fig. 6, shows that overcoupling ($Q_c < Q_i$) can help boosting the efficiency compared to critical coupling ($Q_c = Q_i$) or undercoupling ($Q_c > Q_i$). Both results align with the results in [17]

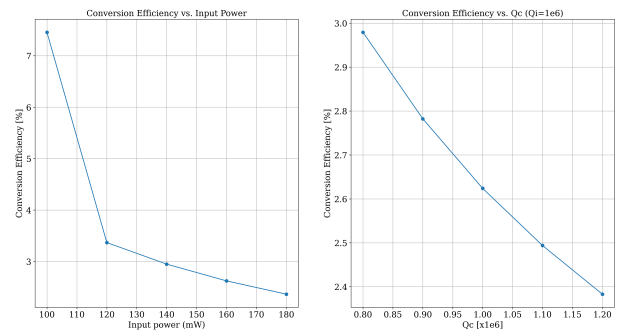


Fig. 6. Conversion efficiency simulated over input pump power and coupling quality factor. It is measured by probing the laser scan transient waveform at index 3600 which corresponds to single soliton state.

Table 1. Simulation Parameters (unless otherwise specified)

Parameters	Numbers
Cavity Radius R	23 μm
Intrinsic Q factor Q_i	1M
Coupling Q factor Q_c	1M
Kerr coefficient γ	$3.2 \text{ W}^{-1}\text{m}^{-1}$
Pump laser power P_{in}	160 mW
Pump laser frequency f_{pmp}	283 THz

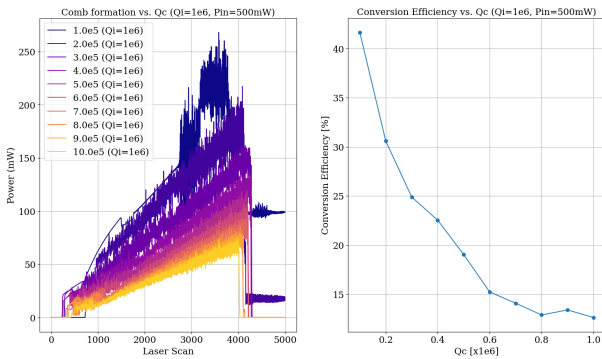


Fig. 7. Soliton formation dynamics and conversion efficiency at strongly overcoupled resonator. Conversion efficiency is measured by probing the laser scan transient waveform at index 3600 which corresponds to single soliton state.

and support the claim that lowering the pump power and over-coupling the resonator is the better design choice in efficiency perspective.

Finally, as suggested in [17], we simulate the dynamics and conversion efficiency of strongly overcoupled micro-resonator. (Figure 7) Here, we increase the pump laser power from 160mW to 500mW as threshold pump power is inversely proportional to the square of Q_t which is dominated by Q_c at an over-coupling case. Well-known equation for threshold power can be approximated as Eq 2, where η is a resonator coupling factor, n and n_2 are refractive and Kerr nonlinear index, A is the mode area and Q_t is a total quality factor by $Q_t^{-1} = Q_c^{-1} + Q_i^{-1}$.

$$P_{th} \simeq 1.54 \frac{\pi}{2} \frac{1}{\eta} \frac{n}{n_2} \frac{\omega}{D_1} \frac{A}{Q_t^2} \quad (2)$$

It is not shown at Fig 7, but we were able to see at $Q_c/Q_i = 0.1$, 160mW was not enough to generate the soliton state. From the graph, it can be seen that $Q_c/Q_i = 0.1$ is able to achieve the conversion efficiency of $> 40\%$. However, as was discussed in [17], it is important to note that conversion efficiency would be limited by bend-induced higher order dispersion and scattering which is not properly captured in the numerical simulation.

5. CONCLUSION AND OUTLOOK

In summary, we simulated the dynamics of Kerr comb generation by using open-source pyLLE package and calculated the conversion efficiency trend against design parameters. Kerr frequency comb has a potential in its inherent advantage of large span and comb count, low noise and coherence. One of the limitations of adopting to the mainstream is the power efficiency, which is studied in this letter. This study shows that at low pump power laser and resonator over-coupling, it is able to achieve high enough conversion efficiency from pump to comb output. Furthermore, comb formation dynamics from laser scanning aligns with the literature, initiated with primary combs to modulation instability state to soliton states.

Future directions may include investigation of application-driven comb optimizations particularly on data communication. Comb-laser based WDM communication is showing promise in upscaling the interconnect bandwidth as it is much easier to increase the number of wavelengths compared to its competitors like DFB arrays. However, it requires much higher wall plug

efficiency and optical power per wavelength to achieve decent operational range for optical communication. With the help of easy-to-use simulator in hand, one would be able to gauge the candidate designs like strongly-overcoupled microring, dispersion engineering and dark solitons in telecom bandwidth.

6. REFERENCES

REFERENCES

- L. Chang, S. Liu, and J. E. Bowers, *Nat. Photonics* **16**, 95 (2022).
- T. J. Kippenberg, A. L. Gaeta, M. Lipson, and M. L. Gorodetsky, *Science* **361**, eaan8083 (2018).
- A. L. Gaeta, M. Lipson, and T. J. Kippenberg, *nature photonics* **13**, 158 (2019).
- T. Herr, V. Brasch, J. D. Jost, C. Y. Wang, N. M. Kondratiev, M. L. Gorodetsky, and T. J. Kippenberg, *Nat. Photonics* **8**, 145 (2014).
- T. Herr, K. Hartinger, J. Riemensberger, C. Wang, E. Gavartin, R. Holzwarth, M. Gorodetsky, and T. Kippenberg, *Nat. photonics* **6**, 480 (2012).
- H. Guo, M. Karpov, E. Lucas, A. Kordts, M. H. Pfeiffer, V. Brasch, G. Lihachev, V. E. Lobanov, M. L. Gorodetsky, and T. J. Kippenberg, *Nat. Phys.* **13**, 94 (2017).
- L. Chang, W. Xie, H. Shu, Q.-F. Yang, B. Shen, A. Boes, J. D. Peters, W. Jin, C. Xiang, S. Liu *et al.*, *Nat. communications* **11**, 1 (2020).
- M. A. Foster, J. S. Levy, O. Kuzucu, K. Saha, M. Lipson, and A. L. Gaeta, *Opt. Express* **19**, 14233 (2011).
- K. Y. Yang, A. D. White, F. Ashtiani, C. Shirpurkar, S. V. Pericherla, L. Chang, H. Song, K. Zou, H. Zhou, K. Pang *et al.*, *arXiv preprint arXiv:2103.14139* (2021).
- A. Rizzo, A. Novick, V. Gopal, B. Y. Kim, X. Ji, S. Daudlin, Y. Okawachi, Q. Cheng, M. Lipson, A. L. Gaeta *et al.*, *arXiv preprint arXiv:2109.10297* (2021).
- P. Marin-Palomo, J. N. Kemal, M. Karpov, A. Kordts, J. Pfeifle, M. H. Pfeiffer, P. Trocha, S. Wolf, V. Brasch, M. H. Anderson *et al.*, *Nature* **546**, 274 (2017).
- D. T. Spencer, T. Drake, T. C. Briles, J. Stone, L. C. Sinclair, C. Fredrick, Q. Li, D. Westly, B. R. Ilic, A. Bluestone *et al.*, *Nature* **557**, 81 (2018).
- A. Rizzo, S. Daudlin, A. Novick, A. James, V. Gopal, V. Murthy, Q. Cheng, B. Y. Kim, X. Ji, Y. Okawachi *et al.*, *IEEE J. Sel. Top. Quantum Electron.* **29**, 1 (2022).
- X. Xue, Y. Xuan, Y. Liu, P.-H. Wang, S. Chen, J. Wang, D. E. Leaird, M. Qi, and A. M. Weiner, *Nat. Photonics* **9**, 594 (2015).
- V. Lobanov, G. Lihachev, T. Kippenberg, and M. Gorodetsky, *Opt. express* **23**, 7713 (2015).
- C. Bao, L. Zhang, A. Matsko, Y. Yan, Z. Zhao, G. Xie, A. M. Agarwal, L. C. Kimerling, J. Michel, L. Maleki *et al.*, *Opt. letters* **39**, 6126 (2014).
- J. K. Jang, Y. Okawachi, Y. Zhao, X. Ji, C. Joshi, M. Lipson, and A. L. Gaeta, *Opt. Lett.* **46**, 3657 (2021).
- G. Moille, Q. Li, X. Lu, and K. Srinivasan, *J. Res. NIST* **124**, 124012 (2019).
- S. Coen and M. Erkintalo, *Opt. letters* **38**, 1790 (2013).
- J. K. Jang, Y. Okawachi, X. Ji, C. Joshi, M. Lipson, and A. L. Gaeta, “Universal conversion efficiency scaling with free-spectral-range for soliton kerr combs,” in *2020 Conference on Lasers and Electro-Optics (CLEO)*, (IEEE, 2020), pp. 1–2.

FULL REFERENCES

1. L. Chang, S. Liu, and J. E. Bowers, "Integrated optical frequency comb technologies," *Nat. Photonics* **16**, 95–108 (2022).
2. T. J. Kippenberg, A. L. Gaeta, M. Lipson, and M. L. Gorodetsky, "Dissipative kerr solitons in optical microresonators," *Science* **361**, eaan8083 (2018).
3. A. L. Gaeta, M. Lipson, and T. J. Kippenberg, "Photonic-chip-based frequency combs," *nature photonics* **13**, 158–169 (2019).
4. T. Herr, V. Brasch, J. D. Jost, C. Y. Wang, N. M. Kondratiev, M. L. Gorodetsky, and T. J. Kippenberg, "Temporal solitons in optical microresonators," *Nat. Photonics* **8**, 145–152 (2014).
5. T. Herr, K. Hartinger, J. Riemensberger, C. Wang, E. Gavartin, R. Holzwarth, M. Gorodetsky, and T. Kippenberg, "Universal formation dynamics and noise of kerr-frequency combs in microresonators," *Nat. photonics* **6**, 480–487 (2012).
6. H. Guo, M. Karpov, E. Lucas, A. Kordts, M. H. Pfeiffer, V. Brasch, G. Lihachev, V. E. Lobanov, M. L. Gorodetsky, and T. J. Kippenberg, "Universal dynamics and deterministic switching of dissipative kerr solitons in optical microresonators," *Nat. Phys.* **13**, 94–102 (2017).
7. L. Chang, W. Xie, H. Shu, Q.-F. Yang, B. Shen, A. Boes, J. D. Peters, W. Jin, C. Xiang, S. Liu *et al.*, "Ultra-efficient frequency comb generation in algaas-on-insulator microresonators," *Nat. communications* **11**, 1–8 (2020).
8. M. A. Foster, J. S. Levy, O. Kuzucu, K. Saha, M. Lipson, and A. L. Gaeta, "Silicon-based monolithic optical frequency comb source," *Opt. Express* **19**, 14233–14239 (2011).
9. K. Y. Yang, A. D. White, F. Ashtiani, C. Shirpurkar, S. V. Pericherla, L. Chang, H. Song, K. Zou, H. Zhou, K. Pang *et al.*, "Inverse-designed multi-dimensional silicon photonic transmitters," arXiv preprint arXiv:2103.14139 (2021).
10. A. Rizzo, A. Novick, V. Gopal, B. Y. Kim, X. Ji, S. Daudlin, Y. Okawachi, Q. Cheng, M. Lipson, A. L. Gaeta *et al.*, "Integrated kerr frequency comb-driven silicon photonic transmitter," arXiv preprint arXiv:2109.10297 (2021).
11. P. Marin-Palomo, J. N. Kemal, M. Karpov, A. Kordts, J. Pfeifle, M. H. Pfeiffer, P. Trocha, S. Wolf, V. Brasch, M. H. Anderson *et al.*, "Microresonator-based solitons for massively parallel coherent optical communications," *Nature* **546**, 274–279 (2017).
12. D. T. Spencer, T. Drake, T. C. Briles, J. Stone, L. C. Sinclair, C. Fredrick, Q. Li, D. Westly, B. R. Ilic, A. Bluestone *et al.*, "An optical-frequency synthesizer using integrated photonics," *Nature* **557**, 81–85 (2018).
13. A. Rizzo, S. Daudlin, A. Novick, A. James, V. Gopal, V. Murthy, Q. Cheng, B. Y. Kim, X. Ji, Y. Okawachi *et al.*, "Petabit-scale silicon photonic interconnects with integrated kerr frequency combs," *IEEE J. Sel. Top. Quantum Electron.* **29**, 1–20 (2022).
14. X. Xue, Y. Xuan, Y. Liu, P.-H. Wang, S. Chen, J. Wang, D. E. Leaird, M. Qi, and A. M. Weiner, "Mode-locked dark pulse kerr combs in normal-dispersion microresonators," *Nat. Photonics* **9**, 594–600 (2015).
15. V. Lobanov, G. Lihachev, T. Kippenberg, and M. Gorodetsky, "Frequency combs and platicons in optical microresonators with normal gvd," *Opt. express* **23**, 7713–7721 (2015).
16. C. Bao, L. Zhang, A. Matsko, Y. Yan, Z. Zhao, G. Xie, A. M. Agarwal, L. C. Kimerling, J. Michel, L. Maleki *et al.*, "Nonlinear conversion efficiency in kerr frequency comb generation," *Opt. letters* **39**, 6126–6129 (2014).
17. J. K. Jang, Y. Okawachi, Y. Zhao, X. Ji, C. Joshi, M. Lipson, and A. L. Gaeta, "Conversion efficiency of soliton kerr combs," *Opt. Lett.* **46**, 3657–3660 (2021).
18. G. Moille, Q. Li, X. Lu, and K. Srinivasan, "pylle: a fast and user friendly lugjato-lefever equation solver," *J. Res. NIST* **124**, 124012 (2019).
19. S. Coen and M. Erkintalo, "Universal scaling laws of kerr frequency combs," *Opt. letters* **38**, 1790–1792 (2013).
20. J. K. Jang, Y. Okawachi, X. Ji, C. Joshi, M. Lipson, and A. L. Gaeta, "Universal conversion efficiency scaling with free-spectral-range for soliton kerr combs," in *2020 Conference on Lasers and Electro-Optics (CLEO)*, (IEEE, 2020), pp. 1–2.